Real time precise GPS constellation and clocks estimation by means of a Kalman filter

D. Laurichesse, L. Cerri, J.P. Berthias, F. Mercier, *Centre National d'Etudes Spatiales, Toulouse, France*

BIOGRAPHY

Denis Laurichesse is a member of the orbit determination service at CNES. He has been in charge of the DIOGENE GPS orbital navigation filter, and is now involved in navigation algorithms for GNSS systems. He is currently in charge of the CNES IGS real time analysis center. He was the co-recipient of the 2009 ION Burka award for his work on phase ambiguity resolution.

Luca Cerri is a member of the orbit determination service at CNES, producing the operational precise orbits for several altimeter missions. He co-chairs the international Precise Orbit Determination science working team for the Ocean Surface Topography missions.

Jean-Paul Berthias is a senior expert in Flight Dynamics and Orbit Determination at CNES.

Flavien Mercier is a member of the orbit determination service at CNES. He participates also to the CNES/CLS IGS analysis center, for the formulation and improvements of the 'GRG' solution. He is a senior expert in GPS processing for precise applications.

ABSTRACT

Real time GNSS orbits and clocks computation is routinely performed, for example, in the framework of the Real Time IGS project. Most of the RTIGS analysis centers use a Kalman filter to compute clocks. To reduce the complexity of the filter, orbits are in general estimated using a least-squares filter based on past data. Orbits are propagated to real-time by a model, such as what is done with predicted IGS orbits (IGUs). By nature, this method is not optimal and limits the precision of the orbits. Sometimes the real time part of IGU orbits is not accurate enough to perform correct narrow-lane ambiguity resolution (which requires an orbit precision of about one quarter the equivalent wavelength which is 10.7 cm for GPS). This problem occurs relatively often with the difficult to model Block IIA type satellites during eclipsing season.

In order to overcome this accuracy problem, a solution is to adjust both orbits and clocks in real time in the Kalman filter. This requires a significant modification of the filter to include the orbital dynamics. This paper presents the details of how this was done on an experimental basis at CNES along with the results.

The paper shows how the computation burden can be significantly reduced by using special optimization techniques in the filter, which allows the execution of a complete Kalman cycle in less than 10 seconds, even on these very large problems (1500+ parameters, 1200 measurements per epoch).

Particular attention has been paid to integer ambiguity resolution. To do so, a zero-difference widelane/narrowlane ambiguity resolution scheme was implemented, following a procedure first presented at ION GNSS 2007, and adapted to the real-time context. Integer ambiguity resolution improves the overall quality of the orbits and clocks, and gives an 'Integer' property to the solution, that is to say the capability for a user receiver to fix its own ambiguities using only the new orbits and clocks.

The paper presents the results in terms of accuracy and availability of the solution. In particular, the paper shows what kind of results can be obtained using freely available real time measurements, like those used in the Real Time IGS project.

The user phase measurement residuals, below the centimeter, are precise enough to fix the zero-difference ambiguities in real-time, thus allowing a positioning on a global scale using an 'integer PPP method', which is a classical PPP approach with integer ambiguities characteristics. The obtained results are at the centimeter level.

The filter can be easily extended to introduce other constellations. Preliminary results on Galileo, using current MGEX streams, show an accuracy of 15 cm 3D RMS.

1. INTRODUCTION

As an IGS Real-Time Service analysis center [4], CNES provides accurate orbits and clocks for GNSS and Glonass (Product prefix CLK9x) on a routine basis. The particularity of the CNES solution is that it implements a technique called 'undifferenced ambiguity resolution' [1]. This technique improves the intrinsic quality of clocks for the IGS Real Time Service. The use of these clocks allows ambiguity resolution on any isolated "user" receiver enabling it to achieve 1 cm horizontal precise point positioning accuracy.

The whole processing is based on a Kalman filter which computes clocks and biases. It uses a priori orbits. In order to mitigate outages that occur on individual orbit solutions (see IGS mails 6524, 6543, 6591, 6615, 6678, 6728, 6736, 6768), a-priori orbits are taken from the following sources:

- IGU (IGS coordinator)
- ESU (ESOC)
- CODE (BERN)
- SGU (IGN)

The useful part of these orbits, i.e. the real-time part, corresponds to the extrapolated part. Figure 1 represents the impact of real-time orbit error on GNSS measurements (computed as ¼ of horizontal orbits errors). In order to correctly fix the N1 ambiguity, this error should be less than a quarter of the N1 wavelength (2.5 cm). It is easy to see that for some satellites (in general eclipsing satellites), this condition is not met.
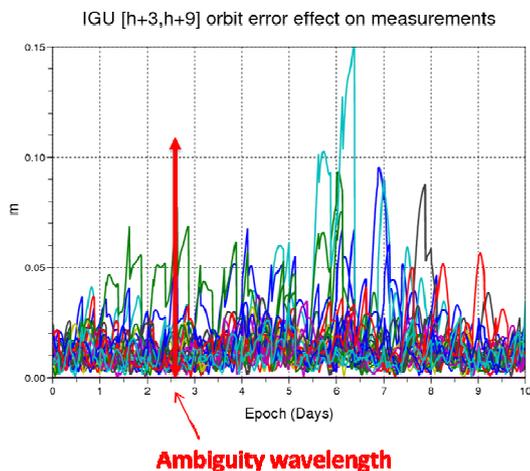
Fig. 1: Orbit error incidence on measurements

Therefore, using a priori extrapolated orbits is not a satisfactory solution. This paper presents an alternate approach where the Kalman filter state is extended to also include orbits, in order to improve accuracy, robustness, and minimize external interfaces.

2. GENERAL ARCHITECTURE

The following figure represents the general architecture of the software:
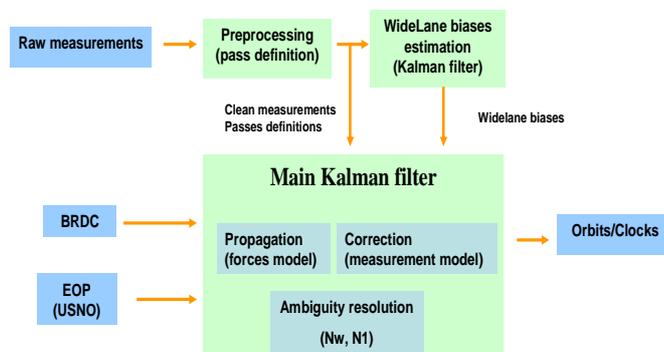
Fig. 2: Architecture of the constellation software

The input data consist in raw measurements, broadcast ephemeris and Earth orientation parameters. Raw measurements are first preprocessed and satellites passes are reconstructed. A specific module based on a Kalman filter handles the computation of satellite widelane biases [1]. The main Kalman filter computes orbits and clocks and handles integer ambiguity resolution of phase measurements.

3. DETAILLED IMPLEMENTATION

3.1 PREPROCESSING

The goal of the preprocessing is, using the 4 pseudo-range and phase measurements (P1, P2, L1, L2), to detect phases jumps and erroneous measurements, in order to construct continuous satellites passes. The algorithm computes certain combinations of observables, and then applies finite time differences at a predefined order to these combinations. An elimination threshold allows the detection of cycle jumps in the combination. The algorithm uses a variable step for finite differences, to maintain continuity of measurements even in presence of important data gaps (up to 1 minute).

Table 1 presents the different combinations which are used and the associated thresholds.

Table 1. Preprocessing combinations

Nom	Combination	Difference order/ Threshold
Widelane	$L_2 - L_1$	4/2.5 cycle
Narrowlane	$\dfrac{\gamma \lambda_1 L_1 - \lambda_2 L_2}{\gamma - 1}$	4/2 m
Ionosphere	$\lambda_1 L_1 - \lambda_2 L_2$	1/10 m
Code	$\dfrac{P_1 + P_2 - (\lambda_1 L_1 + \lambda_2 L_2)}{2} +$ $\dfrac{1 + \gamma}{1 - \gamma}(\lambda_1 L_1 - \lambda_2 L_2)$	1/100 m

3.2 KALMAN FORMULATION

The general formulation of the Kalman filter is of the $P = UDU'$ form, with U an upper triangular matrix and D a squared diagonal matrix. The update of the solution matrix follows the Bierman algorithm [6], while the propagation of the solution uses the Thornton algorithm [5].

Some specific adaptations have been made to these algorithms in order to speed up the process. First, a specific downdating algorithm has been implemented during the update step. This algorithm allows the removal of a single measurement from the solution in only one rank-1 update, without the need to reprocess the entire set of measurements. For the propagation step, the transition matrix has been rearranged in one small full block and one diagonal block, in order to perform the Gram-Schmidt orthogonalization only on the small block. This decreases the time needed by the propagation step by one order of magnitude.

3.3 STATE PROPAGATION

The state propagation involves mainly satellite orbital elements, the other parameters (clocks, tropospheric delay, biases) are modeled as constant from one epoch to another. The satellite motion is computed by integrating a force model. The integrator is a Runge-Kutta (order 6) with a nominal integration step of 60 seconds.

The integration scheme is the following:

$$\begin{cases} y(t_0) = y_0 \\ y' = f(t, y) \end{cases}, \text{ y being the state vector : } y = \begin{pmatrix} p \\ v \end{pmatrix},$$

$$y' = \begin{pmatrix} v \\ a_{tot} \end{pmatrix}$$

The targeted accuracy of the forces in the integrator has been set to 10^{-10} m.s^{-2}. To fulfill this requirement, the following forces have been implemented:

- Geopotential

- 3rd body, solid tides

- Ocean tides

- Relativity

- Solar radiation pressure

The solar radiation pressure is the most difficult force to model. We have chosen a general model, not specifically linked to a particular type of satellite. The satellite is modeled by a sphere with the main force pointing towards the sun. Another force is directed along the satellite Y axis. Finally, to account for unmodeled forces, we also estimate constant and periodic forces expressed in the local orbital frame (radial, along-track, cross-track). These empirical forces are estimated in the Kalman filter. In all, there is an estimation of 11 parameters for each satellite, related to the solar radiation pressure.

Eclipse management is particularly tricky. The force model uses accurate umbra and penumbra computations and during eclipses, the integrator step is reduced to 10 seconds in order to properly account for fast umbra/sun transitions. The dynamical model covariances in the filter also depend of the elevation angle of the sun β: if this angle is close to 0, covariances are multiplied by 5, compared to the setting used out of eclipse.

Table 2 presents in detail the different forces used by the dynamical model:

Table 2. Dynamic model

Force	Amplitude (m/s^2)	Model
Geopotential	0.5	EIGEN RL02 bis Degree and order 12 Secular and periodic terms
Third body	10^{-6}	Moon, Sun, Venus JPL DE 405
Direct solar pressure radiation	10^{-8}	Sphere
Solid tides	10^{-9}	Anelastic Earth model
Y bias	10^{-9}	

Empirical forces	10^{-9}	Orbital frame, constant and 1/rev (sub-solar phased)
Ocean tides	10^{-10}	FES 2004
Relativity	10^{-10}	Schwarzchild

3.4 STATE CORRECTION

The correction step of the Kalman filter involves a modeled measurement set at the current epoch. The measurement combinations used are the ionosphere-free pseudo-range and ionosphere-free phase. The targeted accuracy for the measurement models has been set to 5 mm. To do so, the following terms and models are computed:

Table 3. Measurement model

Model term	Amplitude (m)	Remark
Propagation distance	10^7	Incl. Sagnac effect
Ionosphere	10	Corrected for 1st order using dual frequency measurements
Solid earth tide	0.10	Routine dehanttideinel.f
Phase Wind-Up	0.10	Wu & al.
Troposphere	0.10	Zenithal delay Mapping function: Stanag
Attitude law	0.10	Nominal
Satellites and stations PCV and PCO	0.01	igs08_wwww.atx
Ocean tide loading	0.01	Routine hardisp.f http://www.oso.chalmers.se/~loading
Relativistic effects	0.005	2nd order correction on clocks gravitational time delay

3.5 TIME SCALE

The time scale is given by the clock information contained in the broadcast messages in input. These clocks are processed in the filter as measurements with a loose constraint (noise measurement equals 1 km), which allows to align the clock solution to the GPS broadcast time scale.

3.6 EARTH ORIENTATION, REFERENCE FRAMES

The Earth orientation is given by the polar motion and UT1 values. The polar motion parameters are estimated in the filter. UT1 is not directly observable using GNSS measurements; this is the reason why only its derivative LOD (Length Of Day) is estimated. Polar motion and UT1 are corrected for diurnal and sub-diurnal variations (routine interp.f), while LOD is corrected for zonal tides (routine rg_zont.f). In all, 4 parameters are estimated in the filter. A priori values are taken from the gpsrapid.daily bulletin available at USNO [9].

References frames are ITRF2008 for the terrestrial frame and GCRF for the celestial frame [7]. Time argument is GPS time as given from the measurements. Precession/nutation model is IAU2000A.

3.7 AMBIGUITY RESOLUTION

Ambiguity resolution strategy in the dual-frequency GPS case is documented in [1]. The zero-difference formulation is the following:

$$P_1 = D_1 + \Delta h_p + (e + \Delta \tau_p)$$
$$P_2 = D_2 + \Delta h_p + \gamma(e + \Delta \tau_p)$$
$$\lambda_1 L_1 = D_1 + \lambda_1 W + \Delta h - (e + \Delta \tau) - \lambda_1 N_1$$
$$\lambda_2 L_2 = D_2 + \lambda_2 W + \Delta h - \gamma(e + \Delta \tau) - \lambda_2 N_2$$

with D being the propagation distance, W the wind-up effect, h the clocks, e the ionosphere elongation, N1 and N2 the ambiguities.

Widelane satellites biases μ^j are identified using the following formula:

$$\left\langle \tilde{N}_w \right\rangle = N_w + \mu_i - \mu^j, \text{ where } \tilde{N}_w \text{ is the Melbourne-Wübbena combination.}$$

Widelane resolution uses these biases and an estimation process based on a 30-minute sliding window. This ensures quick and robust widelane estimation. Then, the N1 ambiguity is solved using the phase ionosphere-free measurement according to the following equation:

$$Q_c = D_c + \lambda_c W + h_i - h^j - \lambda_c N_1$$

The resolution is performed directly in the Kalman filter. Depending on the network connectivity, two configurations may arise: ambiguities can either be fixed to any integer value or be forced to a specific integer value [2].

As a by-product, two set of clocks are output: the standard h_p clock which correspond to the clock as defined by IGS, and the 'integer phase clock' h, which allows to perform integer ambiguity resolution on isolated receivers.

3.8 ROBUSTNESS, OUTLIER DETECTION

The outlier detection algorithms are implemented on 4 different levels:

1) The first level involves the raw measurements preprocessing step. This step eliminates the majority of erroneous measurements.

2) The second level aims at eliminating erroneous measurements in the Kalman filter, after an update. A specific threshold (20 m for pseudo-range and 5 cm for phase) is set. Erroneous measurements are eliminated from the filter using the downdating procedure. About 3% of the phase measurements are eliminated during this step at each epoch.

3) The third level aims at detecting an improper behavior of a satellite (in general due to a maneuver). The algorithm computes a sub-problem using only pseudo-range measurements. If certain residual conditions are met, the satellite is declared in anomaly and its parameters are reinitialized.

1) The fourth level detects bad N1 ambiguities. To do so, the number of N1 ambiguities is compared to the number of total measurements. This ratio is monitored and when it falls under a given threshold, ambiguities set for this satellite are reinitialized. Figure 3 shows an example where the number of N1 ambiguities does not follow the evolution of the number of measurements. When such an occurrence is detected, all satellite ambiguities are reinitialized.
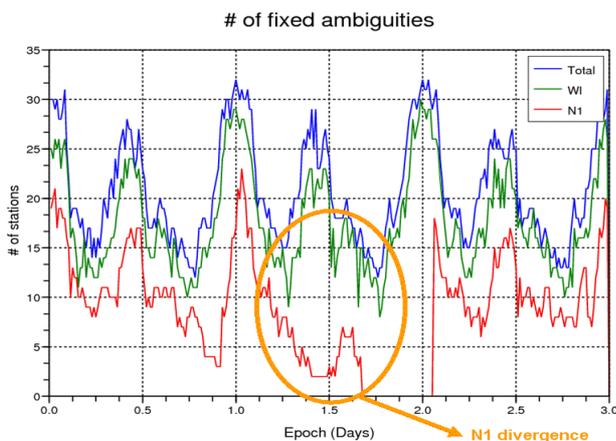
Fig. 3: N1 divergence

3.9 INTEGRITY OF THE SOLUTION

The integrity of the solution is directly given by the formal covariance of the filter and is very basic: The solution is output only when formal covariances are below 5 cm.

3.10 SIZE OF THE PROBLEM, CPU CONSIDERATIONS

Table 4 describes the filter settings, as well as the model noise applied on each parameter (for 60 and 900 seconds step). We assume here that the network contains 32 satellites and 70 stations.

Measurements are the ionosphere-free pseudo-range and phase, with respective noises of 1 m and 1 cm. There are approximately 1600 measurements to update in the filter at each epoch.

Using these settings, the computation time for one step (including propagation and update), is around 10 seconds on a standard machine. In a real-time implementation, this computation time is compatible with a 30-second step for the filter.

ION GNSS 2013, September 16-20, 2013 - Nashville, Tennessee

Table 4. Filter parameterization

Parameter	Quantity	Typical number	Initial covariance	Model noise 900 s	*Model noise 60 s*
Positions	3 per satellite	32*3	1 m	0	0
Velocities	3 per satellite	32*3	0.001 m/s	0	0
Solar pressure coefficient	1 per satellite	32	1	10^{-5}	$2.5\ 10^{-16}$
Y Bias	1 per satellite	32	10^{-13} m/s^2	10^{-13} m/s^2	$2.5\ 10^{-14}$ m/s^2
Radial acceleration (cst, sin, cos)	3 per satellite	32*3	(0, 0, 0) m/s^2	(0, 0, 0) m/s^2	(0, 0, 0) m/s^2
Along-track acceleration (cst, sin, cos)	3 per satellite	32*3	$(10^{-10},\ 10^{-10}, 10^{-10})$ m/s^2	$(10^{-13},\ 10^{-12}, 10^{-12})$ m/s^2	$2.5(10^{-14},\ 10^{-13}, 10^{-13})$ m/s^2
Cross-track acceleration (cst, sin, cos)	3 per satellite	32*3	$(10^{-10},\ 10^{-10}, 10^{-10})$ m/s^2	$(10^{-13},\ 10^{-12}, 10^{-12})$ m/s^2	$2.5(10^{-14},\ 10^{-13}, 10^{-13})$ m/s^2
Polar motion (u, v)	2	2	5.10^{-4} arcsec	5.10^{-5} arcsec	10^{-5} arcsec
UT1	1	1	0	0	0
LOD	1	1	10^{-8} s/s	10^{-11} s/s	10^{-12} s/s
Satellite clock	1 per satellite	32	inf	inf	inf
Satellite bias (code-phase)	1 per satellite	32	1 m	1 mm	0.1 mm
Station clock	1 per station	70	inf	inf	inf
Station bias (code-phase)	1 per station	70	1 m	1 m	1 m
Zenithal tropospheric delay	1 per station	70	0.5 m	1 mm	0.25 mm
Phase ambiguities	12 per station(max)	70*12	1 m	0	0
		1662			

4 REAL-TIME RESULTS

The data used for real-time tests span 10 days from 01/14/3013 to 01/23/2013. They are representative of real-time conditions that can be met in the RTIGS project. The network is composed of around 65 stations, whose measurements can be accessed in real-time using several casters (IGS-IP, GFZ, NrCan, IGN, UNAVCO).

Measurements were pulled from the different casters using the BNC tool [13]. The sampling rate was set to 5 sec. The Kalman filter step was set to 60 sec. The number of measurements processed for this experiment was about 200 millions.

4.1. LOCAL FRAME ORBIT ACCURACY

Orbits computed by the filter are compared to accurate IGS references [8]. Figure 5 shows orbit differences, which can be assimilated as errors in the real-time orbit solutions, projected onto the local orbital reference frame.

Fig. 4: Real-time network

ION GNSS 2013, September 16-20, 2013 - Nashville, Tennessee
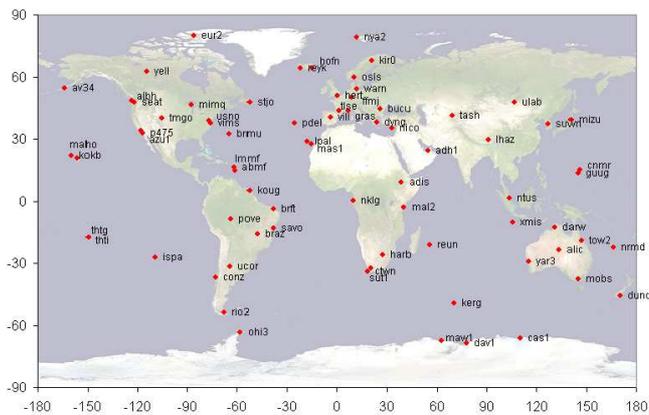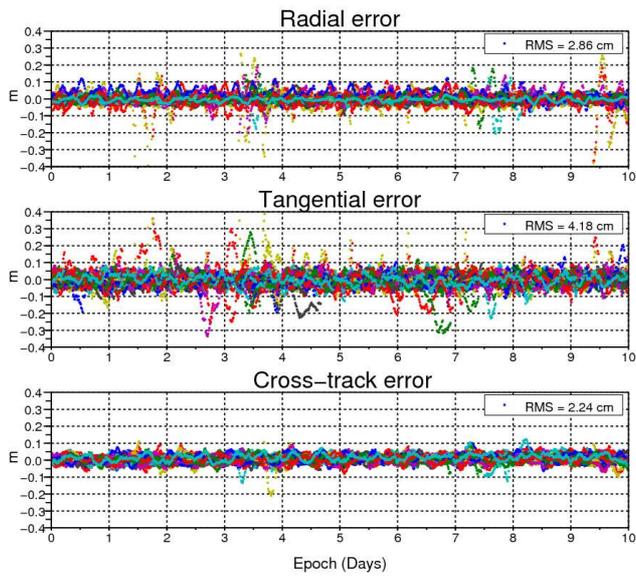
Fig. 5: Orbit error

The RMS are below 5 cm on each axis. The cross-track component is the most accurate without many outliers. The tangential component shows the most erroneous data. After investigation, it appears that these outliers are due to old block IIA satellites in eclipse, which are very difficult to model. The error on the radial component is not significant since it can be absorbed in the clocks.

4.2. 3-D ORBIT ACCURACY

The following figure represents the 3D orbit error. The RMS is quite stable at 3.7 cm. However, eclipsing block II A satellites can locally be erroneous by more than 20 cm.
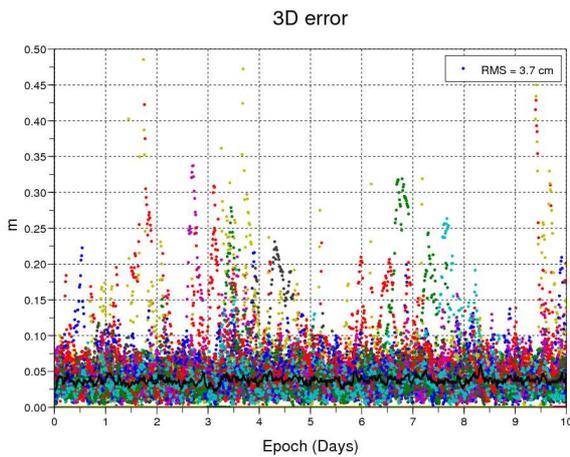
Fig. 6: 3D orbit error

4.3. AMBIGUITY RESOLUTION CONTRIBUTION

The following figure corresponds to the 3D orbit error, when ambiguity resolution is deactivated. RMS is twice the previous RMS. This is more or less the same result as for batch resolutions [3].
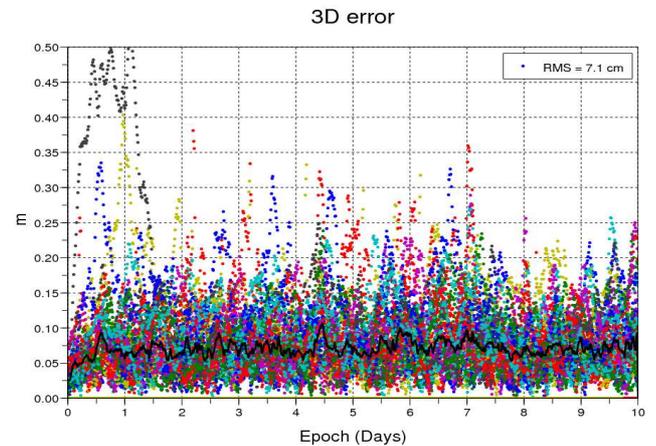
Fig. 7: 3D orbit error without ambiguity resolution

4.4. CLOCK ACCURACY

The following figure represents the clock solution compared to an IGS reference (a constant by satellite and a common value by epoch have been removed). This is equivalent to the combined orbit/clock error, projected on the radial component of the orbit which impacts directly the user error budget.
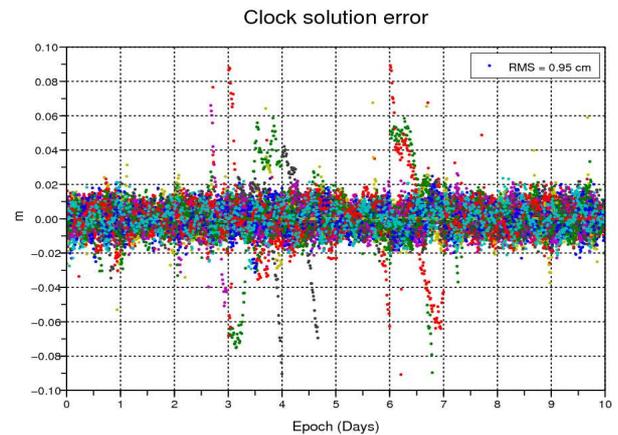
Fig. 8: Clock error

The overall statistic is very good, with an RMS of less than 1 cm. This precision is sufficient to allow ambiguity resolution on an isolated receiver, even though some small errors remain. These errors are directly related to the along-track orbit error (primarily due to eclipsing block IIA satellites).

5. REAL-TIME GALILEO ORBIT DETERMINATION

The first four Galileo satellites used for the In Orbit Validation Phase have been launched in October 2011 and October 2012. They transmit their signals on an operational basis. Thanks to the simultaneous use of these four satellites, ESA has been able to compute the first 'Galileo only' fix in March 2013.

Thanks to the MGEX initiative [10], and using new generation multi-constellation networks like the CNES network REGINA (REseau Gnss pour l'Igs et la NAvigation) and CONGO [11], and new real-time protocols [10], it is possible to collect real-time Galileo measurements.

Figure 9 shows the network of Galileo stations used in this experiment (the GPS network is the standard one described on figure 4):
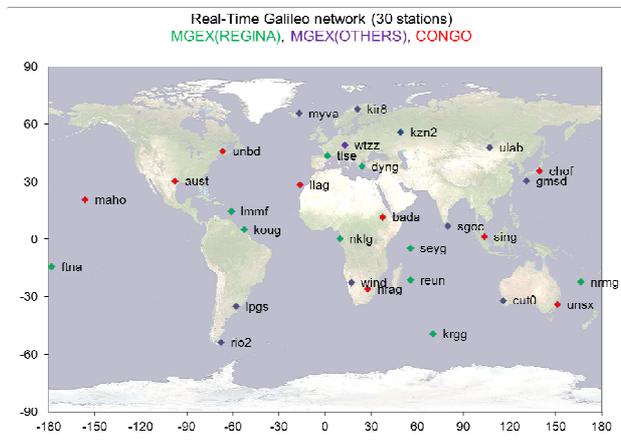
Fig. 9: Real-time Galileo network

The constellation filter was modified to compute Galileo orbits in addition to GPS orbits.

The orbits produced by the real-time filter have been compared to the accurate reference computed in the MGEX framework by the Technical University München [12]. Figure 10 shows the 3D orbit differences between the two solutions, over the 10 days of the experiment. After the first day, once the real-time filter has converged, the 3D RMS orbit difference is about 15 cm. This demonstrates the feasibility of real-time orbit solutions for the combined GPS and GALILEO satellites using currently available real-time networks and tools.
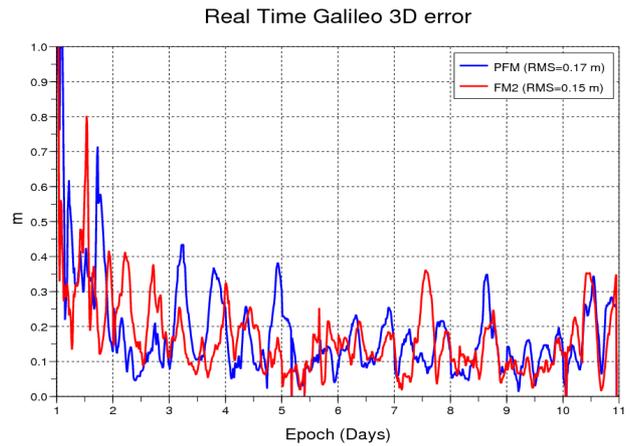
Fig. 10: real-time Galileo 3D error

6. CONCLUSION

We have shown that precise real-time GPS orbit estimation using IGS data, networks and tools as well as a suitable Kalman filter is possible. Results show an accuracy of approximately 3.5 cm 3D RMS. Ambiguity resolution improves the overall accuracy by a factor 2. The filter can be easily extended to introduce other constellations (for example Galileo). Preliminary results, using current MGEX streams, show an accuracy of 15 cm for PFM and FM2 satellites. The new filter will be introduced in the CNES real-time analysis center operational chain.

REFERENCES

[1] D. Laurichesse, F. Mercier, J.P. Berthias, P. Broca, L. Cerri, "Integer Ambiguity Resolution on Undifferenced GPS Phase Measurements and its Application to PPP and Satellite Precise Orbit Determination", Navigation, Journal of the institute of Navigation, Vol. 56, N° 2, Summer 2009

[2] D. Laurichesse, F. Mercier, J.P. Berthias, CNES "Real-time PPP with undifferenced integer ambiguity resolution, experimental results" Proceedings, of the ION GNSS 2010, September 2010, Portland, Oregon

[3] S. Loyer, F. Perosanz, F. Mercier, H. Capdeville, J.C. Marty "Zero-difference GPS ambiguity resolution at CNES–CLS IGS Analysis Center", Journal of Geodesy, November 2012, Volume 86, Issue 11

[4] M. Caissy, G. Weber, L. Agrotis, G. Wübbena, and Manuel Hernandez-Pajares "The IGS Real-time Pilot Project - The Development of Real-time IGS Correction Products for Precise Point Positioning"

Presentations of the EGU11 Vienna, Austria, April 6, 2011

[5] C.L. Thornton,, G.J. Bierman, "Gram-Schmidt Algorithms for Covariance Propagation", International Journal of Control, Volume 25, Issue 2, 1977

[6] G.J. Bierman, "Measurement Updating Using the U-D Factorization", Automatica, Volume 12, Issue 4, July 1976, Pages 375–382

[7] D.D. McCarthy & G. Petit, "IERS Conventions 2003", IERS Technical Note 32, Frankfurt am Main: Verlag des Bundesamts fuer Kartographie und Geodaesie, 2004.

[8] J.M. Dow, R.E. Neilan, G. Gendt, "The International GPS Service (IGS): Celebrating the 10th Anniversary and Looking to the Next Decade," Adv. Space Res. 36 vol. 36, no. 3, pp. 320-326, 2005. doi:10.1016/j.asr.2005.05.125

[9] http://maia.usno.navy.mil/ser7/gpsrapid.daily

[10] MGEX : http://igs.org/mgex/, http://igs.bkg.bund.de/ntrip/mgexobs

[11] Caster CONGO : http://euref-ip.bkg.bund.de

[12] TUM orbits: https://www.iapg.bv.tum.de/mgex

[13] BNC : http://igs.bkg.bund.de/ntrip/download